

Article

Condensed Phase Kinetic Studies of Hydroxynitrates Derived from the Photooxidation of Carene, Limonene, *trans*-Carveol, and Perillic Alcohol

James I. Vesto ¹, Addison B. McAlister ¹, Kathryn A. Wright ², Aaron Huang ¹, Petra R. Baldwin ², Emily J. McLaughlin Sta. Maria ¹, Rebecca Lyn LaLonde ^{1,*} and Anthony J. Carrasquillo ^{2,*}

¹ Department of Chemistry, Reed College, Portland, OR 97202, USA; jivesto@ucdavis.edu (J.I.V.); mcalista@reed.edu (A.B.M.); aahuang@alumni.reed.edu (A.H.); mclaujem@reed.edu (E.J.M.S.M.)
² Department of Chemistry, Williams College, Williamstown, MA 01267, USA; kaw6@williams.edu (K.A.W.); prb4@williams.edu (P.R.B.)
 * Correspondence: rlalonde@reed.edu (R.L.L.); ajc7@williams.edu (A.J.C.)

Abstract: Organic hydroxynitrates (HNs) are key products of hydrocarbon oxidation in the atmosphere. Understanding the fate and processing of these molecules is critical due to their function in the sequestration of NO_x species from the atmosphere and in the formation of secondary organic aerosol. However, the direct study of individual HNs' reactivity has been largely hindered by the lack of authentic standards which has further limited the ability to deconvolute the role of structural features. Herein, we report the kinetic stabilities of six biogenic volatile organic compound-derived HN in acidified single-phase organic/water matrices. Lifetimes for tertiary HNs ranged from 15 min to 6.4 h, whereas secondary HN varied from 56 days to 2.1 years. Product analysis highlights the role that additional non-hydrolysis reactions have in the condensed phase conversion of HNs. This work provides the first evidence for the structural dependence of HN stability in bulk mixed media.

Keywords: hydroxynitrates; organic aerosol; monoterpenes; authentic standards



Citation: Vesto, J.I.; McAlister, A.B.; Wright, K.A.; Huang, A.; Baldwin, P.R.; McLaughlin Sta. Maria, E.J.; LaLonde, R.L.; Carrasquillo, A.J. Condensed Phase Kinetic Studies of Hydroxynitrates Derived from the Photooxidation of Carene, Limonene, *trans*-Carveol, and Perillic Alcohol. *Atmosphere* **2022**, *13*, 592. <https://doi.org/10.3390/atmos13040592>

Academic Editors: Avram Gold and Jason Surratt

Received: 24 February 2022

Accepted: 2 April 2022

Published: 6 April 2022

Publisher's Note: MDPI stays neutral with regard to jurisdictional claims in published maps and institutional affiliations.



Copyright: © 2022 by the authors. Licensee MDPI, Basel, Switzerland. This article is an open access article distributed under the terms and conditions of the Creative Commons Attribution (CC BY) license (<https://creativecommons.org/licenses/by/4.0/>).

1. Introduction

Hydroxynitrates (HNs) are a dominant class of compounds formed from the oxidation of volatile organic compounds (VOCs) by the OH and NO₃ radicals [1–5]. An example oxidation scheme for limonene initiated by the OH radical is shown in Figure 1, where OH adds to one end of the endocyclic double bond, forming an alkyl radical and initiating a series of radical reactions that ultimately lead to a termination at a closed-shell HN. HN formation indirectly impacts O₃ concentrations by sequestering NO_x downstream of their production [6–11]. Further, we estimate that the addition of alcohol and nitrate ester functional groups can depress saturation vapor pressures (C*) by a factor of ~4 × 10⁻⁵ and drive partitioning into the condensed aerosol phase [5,12–15]. While there is some understanding of relative yields of HN from monoterpenes, in the absence of commercially available authentic standards, our understanding of their fate in the condensed phase remains unknown.

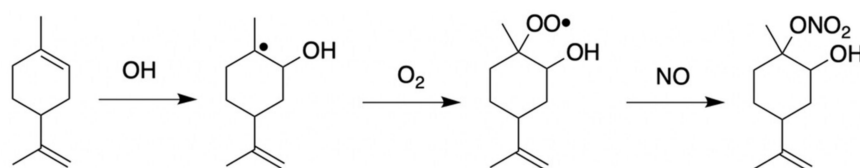


Figure 1. Representative gas phase oxidation reaction of limonene.

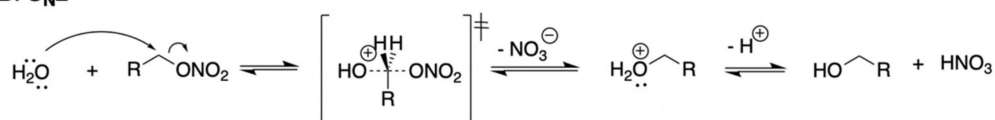
Direct photolysis of HN under ambient conditions is believed to be insignificant while wet and dry deposition are major loss mechanisms in the condensed phase [16,17].

Similarly, neutral and acid-catalyzed hydrolysis of HNs have been shown to be effective degradative pathways in bulk, chamber, and ambient studies [18–31]. Hydrolysis can occur in cloud or fog droplets where liquid water is present, though it has also been observed when liquid water content is low, suggesting a reaction with dissolved water molecules [29]. For highly substituted HN, this mechanism proceeds via an S_N1 -type mechanism where the nitrate ester ($-\text{ONO}_2$) functional group leaves, forming a carbocation intermediate that then undergoes nucleophilic substitution with water, and subsequent deprotonation by NO_3^- to form HNO_3 and a diol (Figure 2A). For less-substituted primary HNs, an S_N2 mechanism is expected to dominate (Figure 2B). In this case, a two-body transition state forms when water attacks the nitrate ester containing carbon center, forcing NO_3^- to leave, which can then deprotonate the added water, yielding a diol and HNO_3 . The product in both cases is the diol; however, the relative stereochemistry differs depending on whether the S_N1 or S_N2 mechanism dominates. It is important to note that for a given substrate, both pathways can occur and the branching ratio between S_N1 and S_N2 will be structure- and matrix-dependent.

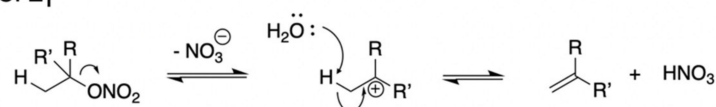
A. S_N1



B. S_N2



C. E_1



D. E_2

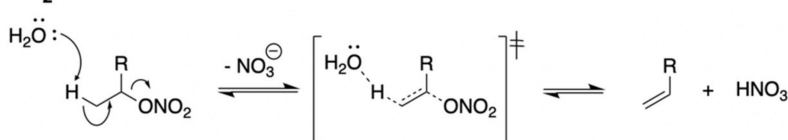


Figure 2. (A) S_N1 mechanism; (B) S_N2 mechanism; (C) E_1 mechanism; (D) E_2 mechanism.

Alternate reaction pathways, such as E_1 and E_2 elimination (Figure 2C,D), as well as carbocation rearrangements, may also be productive for certain substrates. Similar to S_N1 and S_N2 reactions, E_1 and E_2 eliminations proceed by either (1) dissociation of the nitrate ester leaving group, forming a carbocationic intermediate which then undergoes deprotonation at an adjacent carbon to form a π -bond; or (2) simultaneous deprotonation and dissociation of the nitrate ester to form a π -bond. Note that any of the carbocationic intermediates may rearrange to a more stabilized form faster than elimination or substitution. These rearrangement processes are highly structurally dependent and may form products that are structurally distinct from their starting materials. For example, in the synthesis of α -pinene HNs, McKnight observed many rearrangement products [32]. Some of these rearrangement products were nitrated (**1**, **2** and **3**), and others underwent subsequent elimination instead of nucleophilic substitution. Furthermore, none of the expected primary HN structures were observed (Figure 3A). In addition, our previous work on elucidating the products formed from a carene-derived HN showed a high dependence on the matrix (Figure 3B) [31]. In mixed aqueous/organic solvents, *cis*-diol **5** was the dominant product, likely formed via substitution pathways. As the aqueous fraction was increased, a structurally distinct rearrangement product (**6**) became the major product. These results

highlight the need to consider alternate reaction pathways beyond S_N1/S_N2 hydrolysis, particularly in the context of mixed organic/aqueous matrices expected in OA.

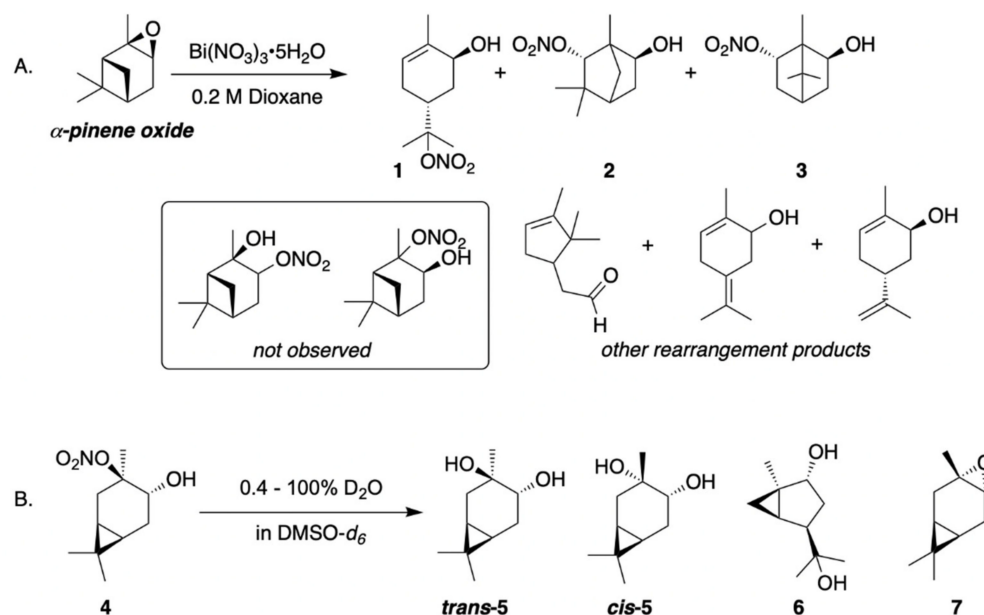


Figure 3. (A) Rearrangement products observed in the synthesis of HN from α -pinene oxide [32]; (B) hydrolysis and rearrangement products observed from carene HN 4 [31].

The molecular structure of the HN has been shown to have a considerable impact on the observed hydrolysis rates for monoterpene-derived HNs. From bulk studies of terpene-derived HNs, increased substitution at the carbon center containing the nitrate group stabilizes the carbocation, resulting in an enhancement in the observed kinetics [18,19,22]. Further, the addition of acid was found to catalyze these bulk phase reactions for secondary and tertiary nitrates [22,25]. Here, protonation of the nitrate ester destabilizes the substrate and enhances the release of HNO_3 , thereby speeding up the kinetics. Chamber studies of isoprene HN were also observed to be acid catalyzed; however, we note that these reactions may not be directly comparable to the bulk aqueous results, as organic aerosol as a “solvent” is quite different from an entirely aqueous solution [29]. The role of solvent in product distribution and branching remains largely unknown.

Here, we present the results from a series of condensed phase experiments examining the stabilities of six terpene-derived HN (Figure 4) in single-phase mixed organic/water matrices with and without the addition of acid. Bulk experiments measuring the degradation or conversion reactions of HN species have almost exclusively been conducted in entirely aqueous media, while hydrolysis reactions in organic matrices (aerosol) at varying RH with low liquid water content have been the focus of chamber studies. While we expected that condensed-phase S_N1 and S_N2 reactions with water would dominate the reactivity of our species, the results from product identification imply that additional pathways of rearrangement and elimination from the carbocation must be considered as well.

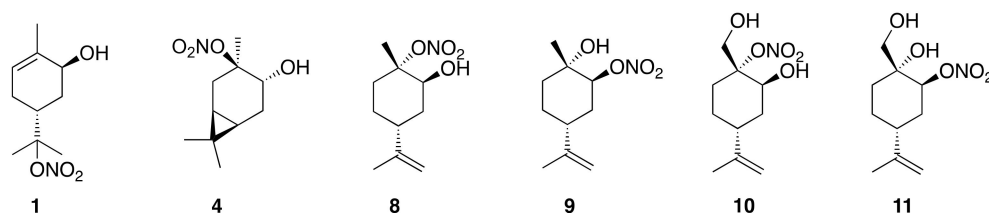


Figure 4. Atmospherically relevant hydroxynitrates in this study.

2. Materials and Methods

2.1. General

All reagents were purchased from commercial sources and were used without further purification unless otherwise noted. Hydroxynitrates and epoxides were prepared according to McKnight (2019) [32]. Diols derived from carene were prepared according to McAlister (2021) [23]. Diols derived from limonene were prepared according to Lu and Lin (2011) [33]. Silica gel TLC plates (60 μm) with a fluorescent indicator (254 nm) were used to monitor the progress of the reactions; they were visualized using UV, anisaldehyde, or KMnO_4 stain. Purification was accomplished with silica gel column chromatography using a Teledyne Isco CombiFlashC Lumen with 25 μm SiliCycle spherical silica gel. The ^1H and ^{13}C NMR spectra were recorded on a Bruker AV400 or AV500 spectrometer and referenced to the protic residue of the deuterated solvents: chloroform-*d* (7.26 ppm), dimethyl sulfoxide-*d*₆ (DMSO-*d*₆, 2.50 ppm), or deuterium oxide (4.79 ppm) unless otherwise noted. Abbreviations include ethyl acetate (EtOAc), ethanol-*d*₆ (EtOD), column volume (CV), retention factor (R_f), singlet (s), doublet (d), doublet of doublets (dd), triplet (t), triplet of triplets (tt), multiplet (m), broad (b), weak (w), medium (m), and strong (s).

2.2. NMR Kinetic Experiments

Three different solvent systems were examined to probe the influence of the aerosol environment on HN conversion: (i) 25% D_2O /DMSO-*d*₆, (ii) acidified 25% D_2O /DMSO-*d*₆, and (iii) acidified 25% D_2O /EtOD-*d*₆. A known mass (1–2 mg) of internal standard, 1-bromo-4-chlorobenzene, 1,2,3-trimethoxybenzene, or dimethyl-2-silapentane-5-sulfonate sodium salt, was dissolved in the appropriate mixture. For acidified experiments, 5 molar equivalents (with respect to HN) of D_2SO_4 were added to the solution and mixed. This solution (0.7 mL) was transferred to an NMR tube, then inserted into the NMR probe preheated to the desired equilibrated temperature (25–80 °C). The instrument was locked and shimmed using this solution, and a pseudo-2D NMR experiment was created using the zg2d pulse sequence to record ^1H NMR spectra at constant time intervals. The time between acquisitions (d20) and number of acquisitions (td) was set to obtain the desired reaction time length (30 min–12 h). Reactions were run until at least 10% of the starting HN had degraded, which varied significantly depending on the structure. For HN structures that reacted too slowly at 30 °C to be monitored in real time, the reactions were run at elevated temperatures and the activation energies (E_a) were determined from the Arrhenius equation (see Supplementary Materials). The solution containing the internal standard was then removed from the probe, mixed with the respective HN (5 mg), and transferred back to the NMR tube. The NMR tube was re-inserted into the probe and data acquisition commenced at the desired temperature for the duration of the experiment. Integration of the internal standard and starting material signals were measured in MestReNova. The starting material ^1H NMR signal intensity (Table S1) was converted to concentration relative to the known concentration of the internal standard, and the consumption modeled using first-order kinetics for the pseudo-2D NMR experiments.

3. Results

3.1. Total Conversion Kinetics of HN in a Mixed Aqueous/Organic Matrix

Six HNs derived from four atmospherically abundant monoterpenes were chosen for this study: carene, limonene, perillic alcohol, and *trans*-carveol (Figure 4). Additionally, secondary and tertiary HNs derived from limonene (2-Lim (9) and 3-Lim (8)) and perillic alcohol (2-Per (11) and 3-Per (10)) were included to assess the role that substitution and additional oxidation plays in conversion kinetics of isomeric compounds. Two additional tertiary HNs from carene (3-Car (4)) and *trans*-carveol (*trans*-Car (1)) provided additional insight into the role of surrounding molecular structure in conversion and product distribution.

To highlight the role of solvent composition on conversion lifetimes, experiments were conducted in a polar aprotic (DMSO-*d*₆) and a polar protic (EtOD-*d*₆) solvent. Additional experiments to determine if acid catalysis is involved in conversion were conducted with

and without the addition of five molar equivalents of D₂SO₄. We examined the stability of each HN in a single-phase mixed 25% D₂O/DMSO-*d*₆ matrix as a proxy for OA where no separate liquid water phase is present. We acknowledge that DMSO is aprotic and ambient OA generally contains an abundance of alcohol and acid moieties; however, this non-nucleophilic solvent provides a suitable foundation for future experiments. At 25%, the concentration of water is large enough such that for hydrolysis, a complete substitution reaction would yield less than a 1% change to the concentration, satisfying the condition for first- or pseudo-first-order kinetics. Further, these C₁₀ HN species have limited aqueous solubility (see Supplementary Materials). Therefore, under these conditions we were able to deconvolute rates of dissolution from the desired rates of conversion.

As HN hydrolysis has been previously shown to be dependent on acid concentration in both the bulk aqueous phase and in chamber-based SOA studies, we also conducted each experiment in two different pH ranges (Table 1). Upon conversion of each HN, HNO₃ is released in solution, thereby changing the pH of the solvent. Buffering the mixed aqueous/organic solutions against the ~30 mM of acid generated during an experiment was challenging, requiring high concentrations of buffer (~3M) that were significant enough to impact the polarity of the solvent mixture. Instead, to gain a qualitative understanding of whether the reactions were susceptible to acid catalysis, parallel experiments were run with and without the addition of 5 molar equivalents of D₂SO₄.

Table 1. Lifetimes (hours) of HN conversion in 25% D₂O/DMSO-*d*₆ with and without the addition of 5 molar equivalents of D₂SO₄. Uncertainties, given in parentheses, represent one standard deviation from triplicate measurements.

HN Structure	Temp (°C)	No Acid (h)	5 Molar Equivalent D ₂ SO ₄ (h)
3-Car (4)	30	0.28 (0.02)	0.25 (0.02)
3-Lim (8)	30	1.45 (0.06)	1.53 (0.1)
2-Lim (9)	80	3.34 (0.3)	2.91 (0.04)
3-Per (10)	50	0.63 (0.03)	0.55 (0.03)
2-Per (11)	80	12.6 (0.6)	9.42 (0.6)

Furthermore, in situ measurements of pH were challenging to conduct in this non-aqueous matrix due to significant fluctuations of up to 1 pH unit. Stabilization timescales were often on the order of 10–20 min, exceeding the observed reaction times. Instead, we measured changes to the pH of bulk 25% aqueous/organic solutions with and without the addition of 5 molar equivalents of H₂SO₄ upon titration with HNO₃. In 25% H₂O/DMSO, the solution pH changed dramatically from pH 9.8 to pH 3.9 with the addition of 0.2 molar equivalents (the range of conversion fit for kinetics, see below), while the addition of 5 molar equivalents of H₂SO₄ prior had a minor buffering effect, maintaining the pH at 1.7 throughout (see Supplementary Materials). In 25% H₂O/ethanol, the solution changed from pH 6.0 to 1.5, while the acidified matrix provided some buffering between pH 0.58–0.41 with the addition of 0.2 equivalents of HNO₃ (see Supplementary Materials). Thus, despite being unable to measure the pH at specified values, a comparison of reaction kinetics with and without the addition of acid provides a qualitative assessment of the role that acid catalysis may have in the degradation of each HN (Table 1).

Real-time monitoring of the reaction progress using NMR allowed for the quantitative tracking of the chemical evolution of our reaction mixtures. Conversion lifetimes were determined by monitoring changes to a ¹H NMR signal unique to the starting material. The concentration of starting material at each time point was determined using peak integrations from an unreactive internal standard over the course of 30 min–12 h at a fixed temperature. Reactions were then modeled using first-order kinetics (Equation (1)) to determine the conversion lifetime (τ Equation (2)):

$$\frac{d[\text{HN}]}{dt} = -k_{\text{obs}}[\text{HN}] \quad (1)$$

$$\tau = \frac{1}{k_{\text{obs}}} \quad (2)$$

where k_{obs} [s^{-1}] is the observed first-order conversion rate constant. While we report conversion lifetimes in lieu of rate constants, note that k_{obs} may be second-order with respect to H_2O for hydrolysis reactions, or third-order if there is an acid-catalyzed mechanism. Reactions were monitored in real time at 30 °C for 3-Car (2), 3-Lim (3), and *trans*-Carv (1), but proceeded too slowly at this temperature for the other species to be completed on reasonable timescales. Instead, we calculated activation energies (E_a) from conversion rates measured at elevated temperatures and estimated the rate constant at 30 °C (Table 2). Finally, we utilized a method of initial rates to determine k_{obs} : for 2-Lim (9), 2-Per (11), and 3-Per (10), this corresponded to 10% conversion of the starting material, however, due to the real-time rapid conversion of 3-Car (4), 3-Lim (8), and *trans*-Carv (1), the initial 25% was fit.

Table 2. Lifetimes (hours) of HN conversion at 30 °C in acidified 25% $\text{D}_2\text{O}/\text{DMSO-}d_6$. Uncertainties, given in parentheses, represent one standard deviation from triplicate measurements.

HN Structure	5 Molar Equivalent D_2SO_4 (h)/30 °C
3-Car (4)	0.25 (0.02)
3-Lim (8)	1.53 (0.1)
2-Lim (9)	1340 (200) ¹
3-Per (10)	5.94 (0.3) ¹
2-Per (11)	18,600 (4000) ¹
<i>trans</i> -Carv (1)	0.37 (0.003) ²

¹ Calculated from E_a measured at elevated temperatures; ² conducted in 10% $\text{D}_2\text{O}/\text{DMSO-}d_6$ at 25 °C.

The decay of the parent HN signal was clear for all the species studied; however, only *trans*-carveol HN (1) and carene HN (2) produced easily identifiable major products that were consistent with E_1 and S_N1 type reactions, respectively. Unlike that previously observed by Wang et. al, where reactions in an aqueous matrix were classified as S_N1 - or S_N2 -type reactions, our observations in a mixed aqueous/organic environment indicate that complex mixtures are formed which appear to be due to a variety of rearrangement, substitution, and elimination reaction pathways available from the carbocation. Hence, the reactions we report are discussed below as rates of consumption of the starting HNs as well as the dynamic spectrum of their products.

3.2. Carene HN

From NMR analyses of 3-Car (4) in 25% $\text{D}_2\text{O}/\text{DMSO-}d_6$, we observed similar reaction products and dynamics (Figure 5) both with (pH 1.7) and without (pH 9.8–3.9 the addition of 5 molar equivalents of D_2SO_4). The conversion lifetimes in both pH ranges were within one standard deviation of triplicate measurements (without acid, 0.28 ± 0.02 h, and with acid, 0.25 ± 0.02 h), indicating that the reaction rate does not have a strong acid-dependence. Further, the expected major and minor diol (5) diastereomeric products ($-\text{CHOH}$, dd at 3.37 and 3.08 ppm, respectively), and rearrangement diol 6 were observed in both cases (Figure 2A) with similar overall yields (*cis*-diol 5 25%, *trans*-diol 5 21%, and rearrangement diol 6 13%). In addition, conversion lifetimes were measured in an acidified polar protic solvent ($\text{EtOD-}d_6$) at 25% D_2O at 30 °C (Table 3). The lifetime in 25% $\text{D}_2\text{O}/\text{EtOD-}d_6$ was more than twice that of the reaction conducted in 25% $\text{D}_2\text{O}/\text{DMSO-}d_6$.

3.3. Limonene HN

We measured the conversion lifetimes of the 2-Lim (9) and 3-Lim (8) isomers to highlight the role of nitrate substitution on the stability of HN isomers. The 3-Lim (8) conversion was fast enough to be monitored in real time at 30 °C with and without the addition of 5 molar equivalents of D_2SO_4 . The addition of the acid did not have a discernable influence on the conversion lifetimes within one standard deviation of triplicate measurements (without acid, 1.45 ± 0.05 h, and with acid, 1.53 ± 0.1 h). The 2-Lim (9)

reacted too slowly at 30 °C to be observed in real time. Instead, the conversion lifetime was estimated by extrapolation from its activation energy measured at elevated temperatures (65–80 °C). We conducted one set of parallel reactions at 80 °C which resulted in the fastest conversion timescale with and without the addition of 5 molar equivalents of D₂SO₄. The conversion lifetimes were 12% faster at lower pH, indicating the presence of acid-catalyzed mechanism(s). To deconvolute the role of a changing pH on conversion kinetics, we only measured the E_a under acidified (pH 1.7) conditions. From the slope of the Arrhenius plot (Figure S2) we measured an E_a of 111 kJ/mol and calculated a conversion lifetime of 55.8 days at 30 °C. As observed for 3-Lim (8), reactions conducted in a 25% D₂O/EtOD-*d*₆ solution at 65 °C were roughly 2–2.5 times slower than in DMSO-*d*₆. Unlike the 3-Car (4), we were unable to clearly identify any of the major products from either 3-Lim (8) or 2-Lim (9). Further, by comparison of ¹H NMR spectra of authentic standards prepared in house, we were unable to definitively identify any of the four expected diol diastereomers from hydrolysis.

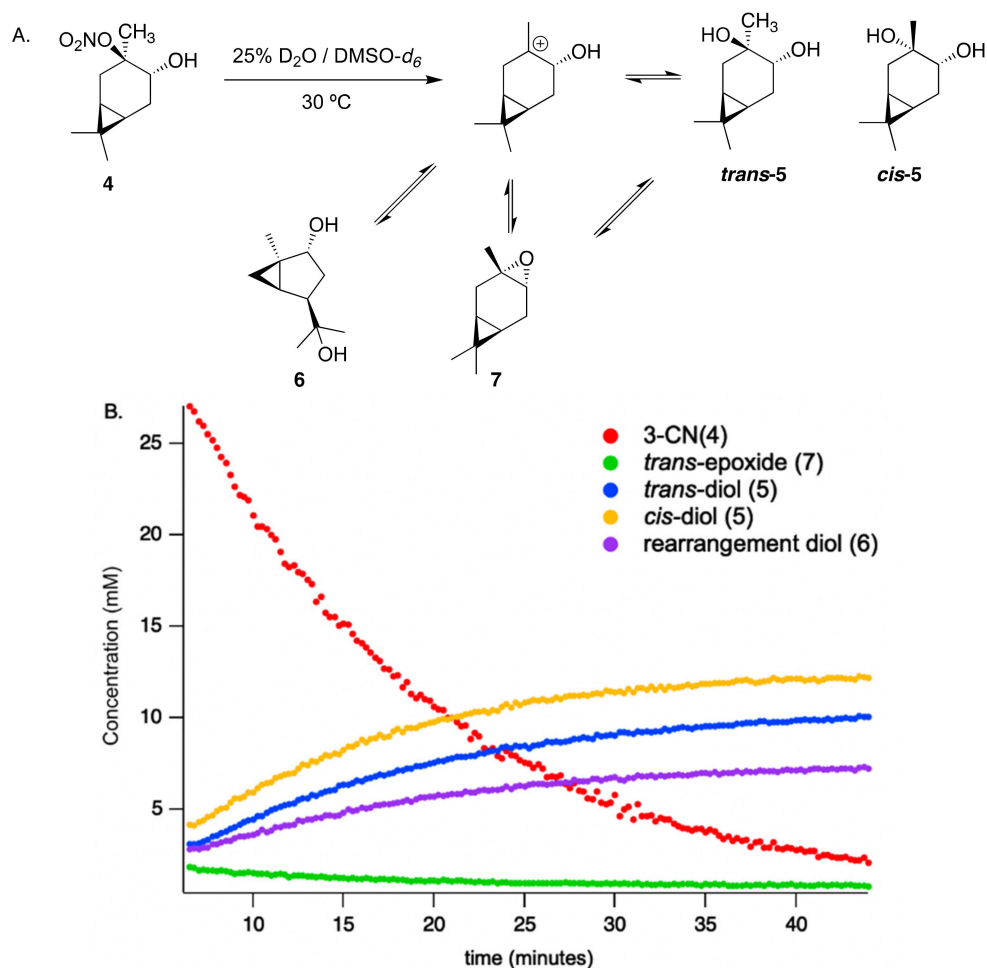


Figure 5. (A) Substitution and rearrangement reaction products from 3-CN (4); (B) time series for the conversion of 3-Car (4) and the formation of the major products in acidified 25% D₂O/DMSO-*d*₆.

3.4. Perillic Alcohol HN

Conversions of both 2-Per (11) and 3-Per (10) were too slow to measure at 30 °C in real time, and instead lifetimes at 30 °C were estimated from E_a determined from reactions at elevated temperatures (65–80 °C). Reactions were conducted in both pH regimes, with and without the addition of acid at 50 and 80 °C for the 3-Per (10) and 2-Per (11), respectively. In both cases we observed a slight decrease in the conversion lifetimes with the addition of acid, indicating that the processes are, in fact, acid-catalyzed (Table 1). From the Arrhenius

plots constructed at 40–60 °C for 3-Per (**10**) and 65–80 °C for 2-Per (**11**), we determined E_a of 101 ± 3 kJ/mole and 136 ± 5 kJ/mole, respectively (Figures S3 and S4). The conversion lifetimes at 30 °C were thus predicted to be 5.93 ± 0.3 h for 3-Per (**10**) and 775 ± 200 days for 2-Per (**11**). Further, consistent with the carene and limonene HN reactions conducted in acidified 25% D₂O/EtOD-*d*₆, conversion was slower by a factor of 2–3. In contrast to the 3-Car (**4**), the NMR analyses of the 2-Per (**11**) and 3-Per (**10**) did not show clear evidence for the major expected diol products. Only the 3-Per (**10**), however, had a clear aldehyde shift (-CHO at 9.3 ppm) that was potentially the result of an elimination reaction to form an enol-**12**, which then tautomerized to the keto form (**12**, Figure 6).

Table 3. Lifetimes (hours) of HN conversion in acidified 25% D₂O/EtOD-*d*₆ and 25% D₂O/DMSO-*d*₆. Uncertainties, given in parentheses, represent one standard deviation from triplicate (DMSO) or duplicate (EtOD) measurements.

HN Structure	Temp (°C)	25% D ₂ O/DMSO- <i>d</i> ₆	25% D ₂ O/EtOD- <i>d</i> ₆
3-Car (4)	30	0.25 (0.02)	0.63 (0.01)
3-Lim (8)	30	1.38 (0.05)	4.72 (0.4)
2-Lim (9)	65	15.87 (0.6)	39.57 (2)
3-Per (10)	50	0.54 (0.03)	1.38 (0.04)
2-Per (11)	65	55.56 (0.6)	143.93 (20)

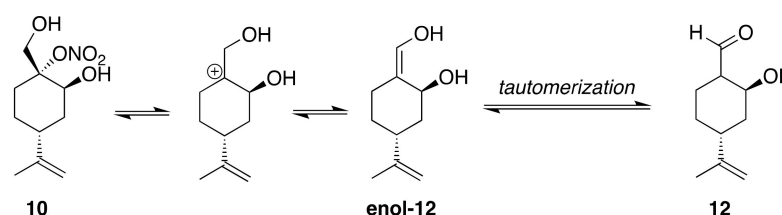


Figure 6. Proposed mechanism of aldehyde formation from 3-Per (**10**).

3.5. *Trans*-Carveol HN

Trans-Carv (**1**) was the most unstable starting material at room temperature in its pure phase. Due to the high instability, the conversion lifetime (22 min) was only investigated in a non-acidified 10% D₂O/DMSO-*d*₆ solution at 25 °C (Figure 7). Based on previous work, we hypothesized that either *trans*-sobrerol or pinol would form from *trans*-Carv (**1**) via inter- or intramolecular S_N1 reactions [25,34]. However, under our reaction conditions, complete E₁ elimination proceeded over the course of 60 min to produce *trans*-carveol with a yield of 90%. While there were other minor products present in the reaction mixture, we did not detect *trans*-sobrerol or pinol in our NMR analyses.

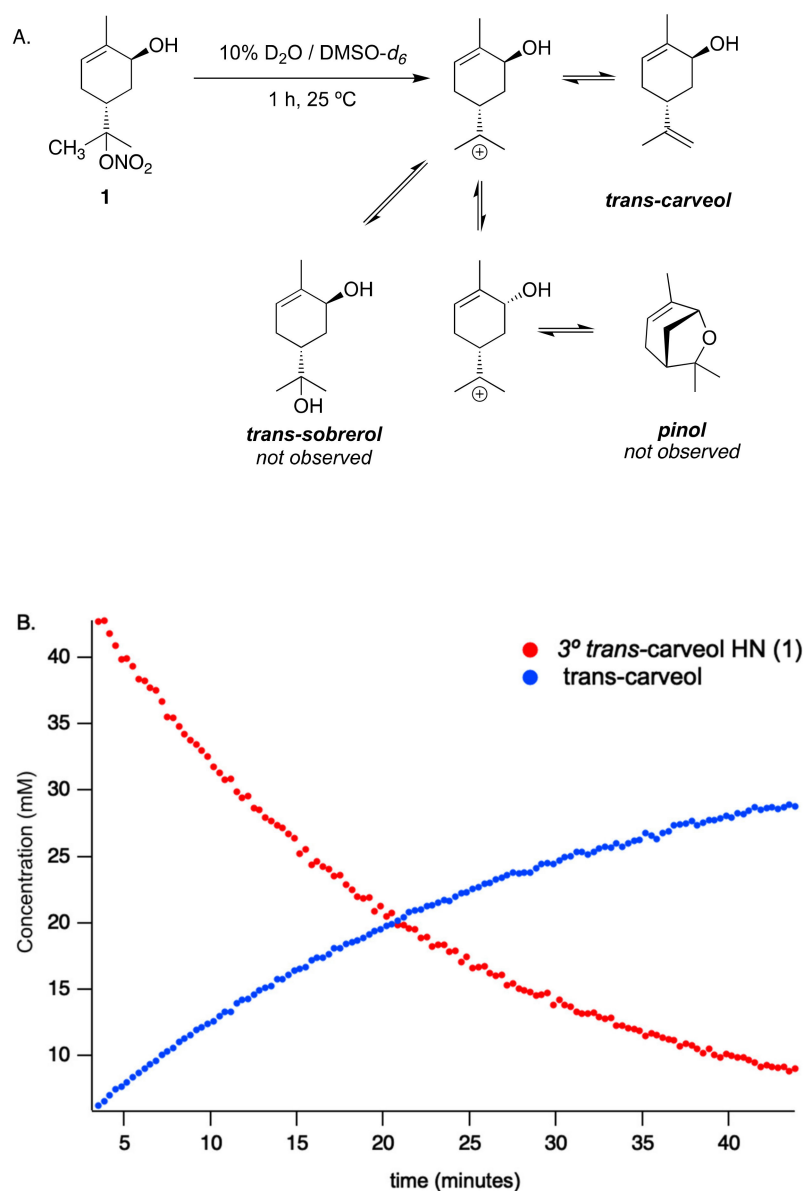


Figure 7. (A) Elimination and substitution reactions of *trans*-Carv (1); (B) time series for the conversion of *trans*-Carv (1) and the formation of *trans*-carveol in 10% D₂O/DMSO-*d*₆ at 25 °C.

4. Discussion

Overall, the rate constants of all secondary species were slower than those of the tertiary compounds, as expected from the enhanced stabilization of the carbocation intermediate on a more highly substituted carbon center. Using the E_a s determined above, we estimated that conversion lifetimes at 30 °C and pH 1.7 were, on average, 3–4 orders of magnitude shorter for the tertiary HN than the secondary species. Among the tertiary species, we observed a relative ordering of conversion rates, 3-Car (4) < 3-Lim (8) < 3-Per (10), which is driven by the molecular structure. The difference in structure between 3-Per (10) and 3-Lim (8) is the presence of an additional alcohol group on the adjacent carbon. This moiety has the effect of further stabilizing the nitrate group through intramolecular hydrogen bonding, resulting in longer conversion lifetimes over limonene HN. This same trend is observed for the secondary 2-Lim (9) and 2-Per (11). The 3-Car (4), on the other hand, is unique among this group as a bicyclic structure that exhibits additional ring strain on the carbon which bears the nitrate group. As a result, there is an enhancement in the effectiveness of the nitrate ester in leaving. The lifetimes from our study were, on average,

longer than those measured for bulk-phase aqueous reactions of other biogenically-derived HNs by up to an order of magnitude.

In our previous investigations of 3-Car (**4**), we saw clear evidence for carene epoxide (**7**), which was confirmed by comparison to an authentic standard (dt at 0.40 and 0.32 ppm). At low concentrations of water (8.4% D₂O), the epoxide (**7**) was the dominant product early in the reaction [23]. Its concentration peaked and decayed rapidly over the last half of the reaction (Figure S9). At 12 min, corresponding to 40% conversion of the starting material, the epoxide (**7**) stopped accumulating and began to decay. As the rate of epoxide (**7**) formation began to slow, the rate of diol (*cis*-**5**) formation concomitantly increased to a yield of 46%. Coincidentally, the second diol (*trans*-**5**) signature (dd, 3.08 ppm) began to form, presumably due to the hydrolysis of the epoxide (**7**), reaching an overall yield of 10% as the epoxide signal decayed. The initial induction period for diol (*trans*-**5**) formation is likely due to competitive formation of epoxide (**7**) and its subsequent hydrolysis (Figure S9). At higher concentrations of water (Figure 5B), the reaction progression is faster; while the initial conditions still favored the formation of the epoxide (**7**), the peak concentration is prior to the start of data acquisition. This observation correlates with the difference in dielectric constants of DMSO-*d*₆, which is roughly twice that of EtOD-*d*₆, which may indicate that the carbocationic intermediate is less stabilized and hence results in slower reaction kinetics. We note that the product yields are also slightly different (*cis*-diol 7%, *trans*-diol 27%, rearrangement 26%). This observation is consistent with our previous findings that the polarity of the matrix impacts the relative rates of carbocation substitution and rearrangement.

In the analogous studies of 2-Lim (**9**) and 3-Lim (**8**) in 100% D₂O, both isomers were observed to undergo acid-catalyzed reactions that were significantly faster than those observed here (5.7–6.6 min at pH 0.33–2.38 for 3-Lim (**8**) and 9.8 days at pH 0.33 for 2-Lim (**9**)) [22]. Together, these observations suggest that the mechanisms are different between the two systems and are thus strongly dependent on the solvent composition. Further, we were unable to identify any of the major hydrolysis products expected and previously identified by Wang [22]. Together, these observations imply that the HN conversion mechanisms in this mixed aqueous/organic environment are different from those which dominate in an entirely aqueous solution. Further, while the exact products and conversion mechanism(s) remain unknown, the first-order kinetic behavior of these systems supports a dominant process that is unimolecular. Additional work to characterize the products is needed to better determine the dominant mechanisms.

5. Conclusions

The results from this work provide the first evidence for the structural dependence of HN stability and reactivity in mixed condensed-phase aqueous–organic matrices. The observed kinetics indicate that, under ambient conditions, tertiary species may undergo a rapid transformation on timescales < 7 h, while secondary species may remain stable on timescales well beyond the lifetime of an average aerosol particle. These lifetimes are far longer on average than expected based on past studies. However, our results only represent those from a particular set of conditions and highlight the need for more targeted studies aimed at identifying the role of solvent/aerosol composition on conversion lifetime. Finally, we unexpectedly observed the predicted hydrolysis product from only one of the six HNs in this study in contrast to previous studies conducted in 100% water. The identities of the products from the other five HNs are unknown, and their chemical structure will have a direct influence on their physiochemical properties, particularly relating to reactivity with oxidants (OH, NO₃, or O₃) or volatilization from the aerosol phase. These, in turn, may impact bulk aerosol properties and particle size. Product identification and the study of their respective properties and reactivities will be the focus of future work. Further, the contrast in our observed products for *trans*-carveol HN with the work of Rindelaub and Bleier further highlights the role of the surrounding matrix on product formation [25,34].

This motivates future investigations into the role of RH and water concentration on non-hydrolysis pathways for the fate of HN.

Supplementary Materials: The following supporting information can be downloaded at: <https://www.mdpi.com/article/10.3390/atmos13040592/s1>, pH studies of mixed water/organic solvents, Arrhenius plots, diol synthetic procedures, diol and HN solubility studies, and NMR progression stacks.

Author Contributions: Conceptualization, R.L.L. and A.J.C.; methodology, R.L.L., A.J.C., A.B.M., J.I.V. and K.A.W.; validation, R.L.L. and A.J.C.; formal analysis, A.J.C., R.L.L., A.B.M., K.A.W. and J.I.V.; investigation, R.L.L., A.J.C., A.B.M., J.I.V., A.H., K.A.W., E.J.M.S.M. and P.R.B.; resources, R.L.L. and A.J.C.; data curation, R.L.L., A.J.C. and J.I.V.; writing—original draft preparation, A.J.C. and R.L.L.; writing—review and editing, R.L.L., A.J.C., K.A.W., E.J.M.S.M., J.I.V. and A.B.M.; supervision, R.L.L. and A.J.C.; project administration, R.L.L. and A.J.C. All authors have read and agreed to the published version of the manuscript.

Funding: This research received no external funding.

Institutional Review Board Statement: Not applicable.

Informed Consent Statement: Not applicable.

Acknowledgments: Williams College and Reed College for Startup Funding. Nathan P. Cook for his assistance with NMR operation at Williams College.

Conflicts of Interest: The authors declare no conflict of interest.

References

1. Wängberg, I.; Barnes, I.; Becker, K.H. Product and Mechanistic Study of the Reaction of NO₃ Radicals with α - Pinene. *Environ. Sci. Technol.* **1997**, *31*, 2130–2135. [[CrossRef](#)]
2. Hallquist, M.; Wängberg, I.; Ljungström, E.; Barnes, I.; Becker, K.H. Aerosol and Product Yields from NO₃ Radical-Initiated Oxidation of Selected Monoterpenes. *Environ. Sci. Technol.* **1999**, *33*, 553–559. [[CrossRef](#)]
3. Spittler, M.; Barnes, I.; Bejan, I.; Brockmann, K.J.; Benter, T.; Wirtz, K. Reactions of NO₃ Radicals with Limonene and α -Pinene: Product and SOA Formation. *Atmos. Environ.* **2006**, *40*, 116–127. [[CrossRef](#)]
4. Matsunaga, A.; Docherty, K.S.; Lim, Y.B.; Ziemann, P.J. Composition and Yields of Secondary Organic Aerosol Formed from OH Radical-Initiated Reactions of Linear Alkenes in the Presence of NO_x: Modeling and Measurements. *Atmos. Environ.* **2009**, *43*, 1349–1357. [[CrossRef](#)]
5. Kroll, J.H.; Seinfeld, J.H. Chemistry of Secondary Organic Aerosol: Formation and Evolution of Low-Volatility Organics in the Atmosphere. *Atmos. Environ.* **2008**, *42*, 3593–3624. [[CrossRef](#)]
6. Fiore, A.M.; Horowitz, L.W.; Purves, D.W.; Levy, H.; Evans, M.J.; Wang, Y.; Li, Q.; Yantosca, R.M. Evaluating the Contribution of Changes in Isoprene Emissions to Surface Ozone Trends over the Eastern United States. *J. Geophys. Res. Atmos.* **2005**, *110*, 1–13. [[CrossRef](#)]
7. Von Kuhlmann, R.; Lawrence, M.G.; Pöschl, U.; Crutzen, P.J. Sensitivities in Global Scale Modeling of Isoprene. *Atmos. Chem. Phys.* **2004**, *4*, 1–17. [[CrossRef](#)]
8. Horowitz, L.W.; Fiore, A.M.; Milly, G.P.; Cohen, R.C.; Perring, A.; Wooldridge, P.J.; Hess, P.G.; Emmons, L.K.; Lamarque, J.F. Observational Constraints on the Chemistry of Isoprene Nitrates over the Eastern United States. *J. Geophys. Res. Atmos.* **2007**, *112*, 1–13. [[CrossRef](#)]
9. Ayres, B.R.; Allen, H.M.; Draper, D.C.; Brown, S.S.; Wild, R.J.; Jimenez, J.L.; Day, D.A.; Campuzano-Jost, P.; Hu, W.; de Gouw, J.; et al. Organic nitrate aerosol formation via NO₃⁺ biogenic volatile organic compounds in the southeastern United States. *Atmos. Chem. Phys.* **2015**, *15*, 13377–13392. [[CrossRef](#)]
10. Pye, H.O.T.; Luecken, D.J.; Xu, L.; Boyd, C.M.; Ng, N.L.; Baker, K.R.; Ayres, B.R.; Bash, J.; Baumann, K.; Carter, W.P.L.; et al. Modeling the Current and Future Roles of Particulate Organic Nitrates in the Southeastern United States. *Environ. Sci. Technol.* **2015**, *49*, 14195–14203. [[CrossRef](#)]
11. Fisher, J.A.; Jacob, D.J.; Travis, K.R.; Kim, P.S.; Marais, E.A.; Miller, C.C.; Yu, K.; Zhu, L.; Yantosca, R.M.; Sulprizio, M.P.; et al. Organic nitrate chemistry and its implications for nitrogen budgets in an isoprene- and monoterpene-rich atmosphere: Constraints from aircraft (SEAC4RS) and ground-based (SOAS) observations in the Southeast US. *Atmos. Chem. Phys.* **2016**, *16*, 5969–5991. [[CrossRef](#)]
12. Perring, A.E.; Pusede, S.E.; Cohen, R.C. An Observational Perspective on the Atmospheric Impacts of Alkyl and Multifunctional Nitrates on Ozone and Secondary Organic Aerosol. *Chem. Rev.* **2013**, *113*, 5848–5870. [[CrossRef](#)]
13. Rollins, A.W.; Smith, J.D.; Wilson, K.R.; Cohen, R.C. Real Time in Situ Detection of Organic Nitrates in Atmospheric Aerosols. *Environ. Sci. Technol.* **2010**, *44*, 5540–5545. [[CrossRef](#)]

14. Xu, L.; Suresh, S.; Guo, H.; Weber, R.J.; Ng, N.L. Aerosol Characterization over the Southeastern United States Using High-Resolution Aerosol Mass Spectrometry: Spatial and Seasonal Variation of Aerosol Composition and Sources with a Focus on Organic Nitrates. *Atmos. Chem. Phys.* **2015**, *15*, 7307–7336. [[CrossRef](#)]
15. Rollins, A.W.; Pusede, S.; Wooldridge, P.; Min, K.E.; Gentner, D.R.; Goldstein, A.H.; Liu, S.; Day, D.A.; Russell, L.M.; Rubitschun, C.L.; et al. Gas/Particle Partitioning of Total Alkyl Nitrates Observed with TD-LIF in Bakersfield. *J. Geophys. Res. Atmos.* **2013**, *118*, 6651–6662. [[CrossRef](#)]
16. Zare, A.; Romer, P.S.; Nguyen, T.; Keutsch, F.N.; Skog, K.; Cohen, R.C. A Comprehensive Organic Nitrate Chemistry: Insights into the Lifetime of Atmospheric Organic Nitrates. *Atmos. Chem. Phys.* **2018**, *18*, 15419–15436. [[CrossRef](#)]
17. Romonosky, D.E.; Nguyen, L.Q.; Shemesh, D.; Nguyen, T.B.; Epstein, S.A.; Martin, D.B.C.; Vanderwal, C.D.; Gerber, R.B.; Nizkorodov, S.A. Absorption Spectra and Aqueous Photochemistry of β -Hydroxyalkyl Nitrates of Atmospheric Interest. *Mol. Phys.* **2015**, *113*, 2179–2190. [[CrossRef](#)]
18. Hu, K.S.; Darer, A.I.; Elrod, M.J. Thermodynamics and Kinetics of the Hydrolysis of Atmospherically Relevant Organonitrates and Organosulfates. *Atmos. Chem. Phys.* **2011**, *11*, 8307–8320. [[CrossRef](#)]
19. Darer, A.I.; Cole-Filipiak, N.C.; O'Connor, A.E.; Elrod, M.J. Formation and Stability of Atmospherically Relevant Isoprene-Derived Organosulfates and Organonitrates. *Environ. Sci. Technol.* **2011**, *45*, 1895–1902. [[CrossRef](#)]
20. Bean, J.K.; Hildebrandt Ruiz, L. Gas-Particle Partitioning and Hydrolysis of Organic Nitrates Formed from the Oxidation of α -Pinene in Environmental Chamber Experiments. *Atmos. Chem. Phys.* **2016**, *16*, 2175–2184. [[CrossRef](#)]
21. Sato, K. Detection of Nitrooxypolyols in Secondary Organic Aerosol Formed from the Photooxidation of Conjugated Dienes under High-NO_x Conditions. *Atmos. Environ.* **2008**, *42*, 6851–6861. [[CrossRef](#)]
22. Wang, Y.; Piletic, I.R.; Takeuchi, M.; Xu, T.; France, S.; Ng, N.L. Synthesis and Hydrolysis of Atmospherically Relevant Monoterpene-Derived Organic Nitrates. *Environ. Sci. Technol.* **2021**, *55*, 14595–14606. [[CrossRef](#)] [[PubMed](#)]
23. McAlister, A.B.; Vesto, J.I.; Huang, A.; Wright, K.A.; Emily, E.J.; Bailey, G.M.; Kretekos, N.P.; Baldwin, P.R.; Carrasquillo, A.J.; Lalonde, R.L. Reactivity of a Carene-Derived Hydroxynitrate in Mixed Organic/Aqueous Matrices: Applying Synthetic Chemistry to Product Identification and Mechanistic Implications. *Atmosphere* **2021**, *12*, 1617. [[CrossRef](#)]
24. Morales, A.C.; Jayarathne, T.; Slade, J.H.; Laskin, A.; Shepson, P.B. The Production and Hydrolysis of Organic Nitrates from OH Radical Oxidation of β -Ocimene. *Atmos. Chem. Phys.* **2021**, *21*, 129–145. [[CrossRef](#)]
25. Rindelaub, J.D.; Borca, C.H.; Hostetler, M.A.; Slade, J.H.; Lipton, M.A.; Slipchenko, L.V.; Shepson, P.B. The Acid-Catalyzed Hydrolysis of an α -Pinene-Derived Organic Nitrate: Kinetics, Products, Reaction Mechanisms, and Atmospheric Impact. *Atmos. Chem. Phys.* **2016**, *16*, 15425–15432. [[CrossRef](#)]
26. Rindelaub, J.D.; McAvey, K.M.; Shepson, P.B. The Photochemical Production of Organic Nitrates from α -Pinene and Loss via Acid-Dependent Particle Phase Hydrolysis. *Atmos. Environ.* **2015**, *100*, 193–201. [[CrossRef](#)]
27. Jacobs, M.I.; Burke, W.J.; Elrod, M.J. Kinetics of the Reactions of Isoprene-Derived Hydroxynitrates: Gas Phase Epoxide Formation and Solution Phase Hydrolysis. *Atmos. Chem. Phys.* **2014**, *14*, 8933–8946. [[CrossRef](#)]
28. Cortés, D.A.; Elrod, M.J. Kinetics of the Aqueous Phase Reactions of Atmospherically Relevant Monoterpene Epoxides. *J. Phys. Chem. A* **2017**, *121*, 9297–9305. [[CrossRef](#)]
29. Vasquez, K.T.; Crounse, J.D.; Schulze, B.C.; Bates, K.H.; Teng, A.P.; Xu, L.; Allen, H.M.; Wennberg, P.O. Rapid Hydrolysis of Tertiary Isoprene Nitrate Efficiently Removes NO_x from the Atmosphere. *Proc. Natl. Acad. Sci. USA* **2021**, *117*, 33011–33016. [[CrossRef](#)]
30. Takeuchi, M.; Ng, N.L. Chemical Composition and Hydrolysis of Organic Nitrate Aerosol Formed from Hydroxyl and Nitrate Radical Oxidation of α -Pinene and β -Pinene. *Atmos. Chem. Phys.* **2019**, *19*, 12749–12766. [[CrossRef](#)]
31. Boyd, C.M.; Sanchez, J.; Xu, L.; Eugene, A.J.; Nah, T.; Tuet, W.Y.; Guzman, M.I.; Ng, N.L. Secondary Organic Aerosol Formation from the β -Pinene+NO₃ System: Effect of Humidity and Peroxy Radical Fate. *Atmos. Chem. Phys.* **2015**, *15*, 7497–7522. [[CrossRef](#)]
32. McKnight, E.A.; Kretekos, N.P.; Owusu, D.; LaLonde, R.L. Technical Note: Preparation and Purification of Atmospherically Relevant Alpha-Hydroxynitrate Esters of Monoterpenes. *Atmos. Chem. Phys.* **2019**, *20*, 4241–4254. [[CrossRef](#)]
33. Lu, T.J.; Lin, C.K. Asymmetric Synthesis of α -Methyl- α -Amino Acids via Diastereoselective Alkylation of (1s)-(+)-3-Carene Derived Tricyclic Iminolactone. *J. Org. Chem.* **2011**, *76*, 1621–1633. [[CrossRef](#)]
34. Bleier, D.B.; Elrod, M.J. Kinetics and Thermodynamics of Atmospherically Relevant Aqueous Phase Reactions of α -Pinene Oxide. *J. Phys. Chem. A* **2013**, *117*, 4223–4232. [[CrossRef](#)]